Clinical, Cosmetic and Investigational Dermatology

Dovepress

open access to scientific and medical research

Open Access Full Text Article

ORIGINAL RESEARCH

# Long Non-Coding RNA B3GALT5-AS1 Suppresses Keloid Progression by Regulating the β-Trcp1-Mediated Ubiquitination of HuR

Wei Ye[1,*], Junwen Lu[1,*], Zuxian Yang[2], Ben Yang[2], Guanya Zhu[2], Chunli Xue[2]

[1]Department of Burn Surgery, the First Clinical Medical College of Guangdong Medical University, Huizhou, 516001, People's Republic of China; [2]Department of Burn Surgery, Huizhou Municipal Central Hospital, Huizhou, 516001, People's Republic of China

*These authors contributed equally to this work

Correspondence: Chunli Xue, Department of Burn Surgery, Huizhou Municipal Central Hospital, No. 41, Eiling North Road, Huicheng District, Huizhou, 516001, People's Republic of China, Email xuechunli2001@163.com



**Background:** lncRNA β-1,3-galactosyltransferase 5-AS1 (B3GALT5-AS1) plays a vital regulatory role in colon and gastric cancers. However, the biological functions and regulatory mechanisms of B3GALT5-AS1 in keloid progression remain unknown. This study aims to investigate the molecular mechanisms in the B3GALT5-AS1-regulated keloid proliferation and invasion.

**Methods:** Secondary mining of the lncRNA sequencing data from GSE158395 was conducted to screen differentially expressed lncRNAs between keloid and normal tissues. MTT, cell migration and invasion assays were performed to detect the effects of B3GALT5-AS1 on keloid fibroblasts (KFs) proliferation and metastasis. The extracellular acidification rate (ECAR) and oxygen consumption rate (OCR) were also determined to evaluate glycolysis in KFs. RNA pull-down and RNA-protein immunoprecipitation assays were used to confirm the interaction between B3GALT5-AS1 and Hu-Antigen R (HuR). Further ubiquitination and rescue experiments were performed to elucidate the regulatory relationship between B3GALT5-AS1 and HuR.

**Results:** B3GALT5-AS1 was significantly down-regulated in keloid tissues and fibroblasts. B3GALT5-AS1 overexpression significantly inhibited KFs proliferation, glycolysis, invasion, and migration and promoted cell apoptosis, whereas silencing B3GALT5-AS1 inhibited these effects. Moreover, B3GALT5-AS1 binds to HuRand reduces its stability through β-Transducin repeats-containing protein 1 (β-Trcp1)-mediated ubiquitination. Overexpression of HuR reversed the inhibition of B3GALT5-AS1 on cell proliferation, migration, and invasion in KFs, where glycolysis pathway was involved.

**Conclusion:** Our findings illustrate that B3GALT5-AS1 has great effect on inhibition of keloid formation, which provides a potential target for keloid therapy.

**Keywords:** B3GALT5-AS1, keloid, fibroblast, HuR, β-Trcp1

## Introduction

Keloid is a highly recurrent benign skin tumor resulting from excessive fibroblast proliferation and progressive extracellular matrix deposition.[1] Although several common strategies, including surgical excision, radiation therapy, steroid injections, and compression therapy, have been applied for preventing and treating keloid, they have been proven to be limited effectiveness and easy relapse.[2,3] Therefore, more attention should be paid to explore the pathogenic mechanisms underlying keloid progression and developing innovative therapeutic strategies.

Long non-coding RNAs (lncRNAs) are a heterogeneous population of RNA molecules that are longer than 200 nucleotides but lack functional open reading frames.[4] Numerous lncRNAs play regulatory effects in diverse biological processes, such as gene transcription, post-transcription, and epigenetic modification, due to the advances of high-throughput sequencing and bioinformatics technologies.[5,6] Moreover, accumulating evidence demonstrated that the aberrant lncRNA expression had been associated with the pathological development of keloid disorder.[7,8] lncRNA

Received: 20 November 2023
Accepted: 21 April 2024
Published: 30 April 2024

H19 up-regulation the proliferation and metastasis of fibroblasts by altering the miR-29a and COL1A1 expression.[9] Moreover, the high HOXA11-AS expression was observed in keloid tissues and fibroblasts, inhibiting cell apoptosis and facilitating angiogenesis via the miR-124-3p/TGFβR1 axis.[10] However, whether other potential lncRNAs can regulate keloid formation remains unknown; thus, ongoing research in the regulatory mechanisms of lncRNAs in keloid pathogenesis is essential for developing diagnostic targets for keloid therapy.

In this study, GEO dataset was used to analyze differentially expressed lncRNAs in keloid tissues compared to normal tissues. A low level of B3GALT5-AS1 was found in keloid tissues, but its function has not been reported yet. We evaluated cell proliferation, invasion, and migration in keloid fibroblasts (KFs) after overexpression or knockdown of B3GALT5-AS1. We found that B3GALT5-AS1 promoted the binding of β-Trcp1 to HuR, leading to the ubiquitination and degradation of HuR. This results in inhibition of cell proliferation and metastasis in KFs. Further, we confirmed the interaction between B3GALT5-AS1 and HuR via characterizing biological features of KFs after overexpression of HuR.

# Materials and Methods

## Acquisition of GEO Sequencing Data

The GSE158395 dataset was downloaded from the NCBI GEO database (http://www. ncbi.nlm.nih.gov/geo). This dataset included lncRNAs sequencing data from four lesion keloid individuals and six health controls. The significant criteria for differential gene expression were set as follows: $|\log_2 FC| > 2$ and $p < 0.05$.

## Isolation of Fibroblasts and Cell Culture

KFs and normal fibroblasts (NFs) were isolated from keloid and adjacent normal tissues. Specifically, the excised fresh keloid specimens and normal skin tissues were immediately rinsed three times with Hank's buffer containing 100 μg/mL penicillin and 100 μg/mL streptomycin. Then they were cut manually on a clean bench. The tissue blocks were preserved and digested with 0.25% trypsin at room temperature for 30 min. The liquid was collected and centrifuged after filtration. The precipitate was re-suspended and maintained in high-glucose Dulbecco's modified Eagle's medium (DMEM; Gibco, Grand Island, USA) supplemented with 10% fetal bovine serum (Gibco) at 37 °C in a 5% $CO_2$ incubator.

## Lentiviruses, Plasmid, and Transfection

The lentiviral expression vectors with shRNA-B3GALT5-AS1 (sh-B3GALT5-AS1) or B3GALT5-AS1 were obtained from Obio (Shanghai, China). The control vector of B3GALT5-AS1-carrying vector served as control group (Ctrl), while the corresponding control vector of sh-B3GALT5-AS1 acted as negative control (NC). These vectors were respectively transfected into HEK293T cells to produce crude lentivirus. The infection efficiency was confirmed using quantitative real-time polymerase chain reaction (qRT-PCR). The coding sequence of HuR was inserted into the pcDNA3.1 vector (Invitrogen) and then transfected into KFs using Lipofectamine 2000 (Invitrogen).

## qRT-PCR

Total RNA was extracted from cells using TRIzol reagents (Invitrogen, Carlsbad, USA) according to the manufacturer's instructions. The cDNA was synthesized using MMLV reverse transcriptase (Promega, Madison, USA). The qPCR was performed with SYBR Green SuperMix (Roche, Basel, Switzerland) using ABI 7900HT PCR System (Applied Biosystems, Foster City, USA). The relative expression was quantified using the 2−ΔΔCT method, with β-actin as an internal standard control. The primers were as follow: B3GALT5-AS1 primers: forward 5' GCGGTTACCCTCATGCTGT 3', reverse 5' CTTGTCCTTCACTTGGCTGC 3'; HuR primers: forward 5' AATTGGCGTGTAATGATGGC 3', reverse 5' CTGAACGATGTCACTGAAAGG 3'; β-actin primers: forward 5' CTCCATCCTGGCCTCGCTGT 3', reverse: 5' ACTAAGTCATAGTCCGCCTAGA 3'; U6 primers: forward 5' CTCGCTTCGGCAGCACA 3', reverse 5' AACGCTTCACGAATTTGCGT 3'; 18S rRNA primers: forward 5' CAGCCACCCGAGATTGAGCA 3', reverse 5' TAGTAGCGACGGGCGGTGTG 3'.

## MTT Assay

The cells were seeded in a 96-well plate at $6\times10^3$ cells/well density. Briefly, 20 μL of 5 mg/mL MTT reagent (Sigma-Aldrich, St Louis, USA) was supplemented into each well at 24, 48, 72, and 96 h, followed by incubation for 4 h at 37 °C. After discarding the supernatants, 100 μL of DMSO solution was added to each well to dissolve formazan crystals. Finally, the absorbance was measured at 490 nm using a microplate reader (Molecular Devices, Sunnyvale, USA).

## Cell Apoptosis Assay

The cells were collected, washed, and re-suspended with 1× binding buffer, and 100 μL cell sample ($1.0\times10^6$ cells/mL) was mixed with Annexin V-FITC and 5 μL of PI (Sigma-Aldrich). The samples were detected and analyzed within 30 min using flow cytometry (Becton Dickinson, Franklin Lakes, USA).

## Cell Invasion Assay

A Transwell chamber coated with Matrigel (Corning, USA) was used to evaluate the invasive ability of fibroblast. The cells were seeded at $2\times10^4$ cells/well density on the upper chamber with 200 μL of non-supplemented DMEM medium or 1 mM 2-DG. Moreover, the lower chamber was filled with DMEM medium supplemented with 10% FBS in 600 μL. After 24 h of cultivation, the cells that crossed the barrier and migrated to the lower chamber were fixed with 4% paraformaldehyde and stained with crystal violets. The images were captured using a digital camera microscope (Olympus, Japan). The number of invaded cells was counted.

## Cell Migration Assay

The cells were seeded into six-well plates ($4\times10^5$ cells/mL) and cultured for 24 h to obtain a confluent cell monolayer. The cell wound scratches were made with a sterile 1 mL pipette tip, and non-adherent cells were removed, followed by incubation with serum-free DMEM medium for 24 h. The cell migration was photographed at 0 and 24 h, and images were captured using a digital camera microscope (Olympus). The migrated area was quantified using IPP 6.0 (Media Cybernetics, USA) software. The results were expressed as the proportion of the scratch area filled with cells.

## Western Blotting Analysis

The cells were collected and lysed with RIPA buffer (Beyotime, Shanghai, China), and the total protein was detected using a BCA protein assay kit (Beyotime). Equal amounts of protein were separated using 10% sodium dodecyl sulfate-polyacrylamide gel electrophoresis (SDS-PAGE) and transferred into polyvinylidene fluoride (PVDF) membranes (Millipore, Schwalbach, Germany). After blocking with 5% milk for 2 h, the membrane was incubated with primary antibodies (1:1000), including anti-HuR antibody (Cell signaling Technology), anti-Ki67 antibody (Abcam), anti-caspase 3 antibody (Abcam), anti-MMP-9 antibody (Abcam), anti-E-cadherin antibody (Abcam), and anti-N-cadherin antibody (Abcam), at 4 °C overnight. Anti-β-actin antibody (1:3000; Cell signaling Technology) acted as an internal control. Subsequently, the membrane was hybridized with an HRP-conjugated secondary antibody (1: 5000; Cell signaling Technology). The signals were determined using chemiluminescence.

## Glucose Uptake Assay and Lactate Production Measurement

After 24 h of seeding in a 96-well plate, cells were treated with 50 μL 2-DG (1 mM) for 15 min. After adding 25 μL stop solution to the well, the mixture was incubated for 1 h at room temperature. Eventually, the luminescence signaling was interrupted using Luminoskan Ascent (Thermo Fisher, USA).

Cells were maintained in a serum-free medium for 24 h for lactate production measurement, followed by examination using a lactate detection kit (Enzyme-linked Biotechnology, Shanghai, China).

## Seahorse Assays

Seahorse assays were performed using the Seahorse XF24 analyzer (Seahorse Bioscience, Agilent). Briefly, cells were seeded into an XF cell culture microplate at a density of $4\times10^4$ cells/well. After 24 h, the extracellular acidification rate

(ECAR) was measured in an XF base medium, followed by sequential additions of Glucose (10 mM), oligomycin (1 μM), and 2-DG (50 mM). The data were analyzed using the Glycolysis Stress Test Report Generator package.

For oxygen consumption rate (OCR) measurement, cells were maintained in an XF base medium containing 10 mM glucose, 1 mM pyruvate, and 2 mM glutamine, followed by sequential additions of oligomycin (1.5 μM), FCCP (1 μM), and Rot/AA (0.5 μM). The data were analyzed using the Cell Mito Stress Test Report Generator package.

## Fluorescence in situ Hybridization (FISH)

Cy3-labeled B3GALT5-AS1 probes were synthesized using RiboBio (Guangzhou, China). The signals were detected using a Fluorescent In situ Hybridization Kit (RiboBio, Guangzhou, China) according to the manufacturer's instructions. The images were captured by fluorescence microscopy with a digital camera (Eclipse E6000; Nikon, Japan).

## Isolation of Nuclear and Cytoplasmic RNA

The nuclear and cytoplasmic RNA in KFs was isolated using a PARIS Kit (Invitrogen, USA) according to the manufacturer's instructions. Then, the subcellular fractions were obtained and analyzed using qRT-PCR. U6 and 18s rRNA were used as nucleus and mRNA controls, respectively.

## RNA Pull-Down and RNA-Protein Immunoprecipitation (RIP) Assay

The RNA pull-down assay was performed using a magnetic RNA-protein pull-down kit (Thermo, MA, USA), according to the manufacturer's introductions. The biotinylated B3GALT5-AS1 probe was mixed with streptavidin magnetic beads and incubated with cell lysates at 4 °C overnight. Then, the protein complex was eluted and analyzed using Western blotting.

RIP was performed using a Magna RNA-binding Protein Immunoprecipitation Kit (Millipore, Bedford, MA, USA) to determine the association between B3GALT5-AS1 and HuR protein. KF cell lysates were collected, incubated with anti-HuR antibody or IgG, and treated with proteinase K. The immunoprecipitated RNAs were isolated with Trizol reagent and analyzed using qRT-PCR assay.

## Cycloheximide-Chase Assay

KFs infected with sh-B3GALT5-AS1 or NC lentiviruses were treated with cycloheximide (CHX, Sigma Aldrich) alone or combined with MG132 or chloroquine (Sigma Aldrich). The HuR protein level was analyzed using Western blotting at 0, 4, 8, and 12 h.

## Ubiquitination Assay

After 12 h of MG132 treatment, the cells were lysed for immunoprecipitation. The cell lysates were collected and incubated with Protein-A/G MagBeads (Yeason, Shanghai, China) and anti-HuR antibody (Cell Signaling Technology) or IgG (Cell Signaling Technology) overnight at 4 °C. The protein complexes were collected and washed. The proteins were analyzed using Western blotting with an anti-ubiquitin antibody (Cell Signaling Technology).

## Co-Immunoprecipitation Assay

The cell lysates were incubated with Protein-A/G MagBeads (Yeason, Shanghai, China) and anti-HuR or anti-β-TrCP1 antibodies (Cell Signaling Technology) overnight at 4 °C. The protein complexes were centrifuged and washed, and the proteins were subjected to Western blotting with anti-HuR or anti-β-Trcp antibodies.

## Statistical Analysis

The data analyses were executed using Student's *t*-test and GraphPad Prism 8.0. The difference between the two groups was determined using Student's *t*-test. A one-way ANOVA test (Tukey multiple comparisons, as recommended by software) was used to analyze differences between more than two groups. All data were presented as the mean ± SD. Statistical differences were considered significant at $*p < 0.05$, $**p < 0.01$ and $***p < 0.001$.

# Results

## B3GALT5-AS1 Was Down-Regulated in Keloid Tissues and KFs

Secondary mining of the RNA sequencing data from GSE158395 was performed to analyze differentially expressed lncRNAs in keloid tissues and normal skin tissues and investigate dysregulated lncRNAs in the pathogenesis of keloid. Therefore, 30 lncRNAs were significantly down-regulated in the four keloid patients than in normal individuals, with B3GALT5-AS1 having a relatively low abundance (Figure 1A). Considering that fibroblasts are the predominant cells attaching to fibrin matrix during the proliferative phase of keloid,[1] we detected the B3GALT5-AS1 expression in fibroblasts using RT-qPCR assay. B3GALT5-AS1 expression was decreased in KFs compared to the NFs group (Figure 1B), illustrating that B3GALT5-AS1 may play a vital role in Keloid progression.

## B3GALT5-AS1 Suppressed KFs Proliferation and Metastasis

KFs were infected with lentiviruses to overexpress or silence B3GALT5-AS1 expression to determine the functions of B3GALT5-AS1 in KFs in vitro. The qRT-PCR results revealed that B3GALT5-AS1-silenced KFs and B3GALT5-AS1-overexpressing KFs were successfully established (Figure 2A). B3GALT5-AS1 overexpression significantly restrained the KF proliferation compared to the control group, whereas B3GALT5-AS1 knockdown increased the cell viability (Figure 2B). Similarly, the migration and invasion ability of KFs was limited after B3GALT5-AS1 overexpression, but these effects could be reversed by silencing B3GALT5-AS1 (Figures 2C and D). Flow cytometry assay discovered that B3GALT5-AS1 up-regulation markedly elevated the percentage of apoptosis cells, whereas B3GALT5-AS1 knockdown decreased the proportion (Figure 2E). After B3GALT5-AS1 up-regulation, tumor proliferative marker (Ki67), migration-associated protein (MMP-9), and epithelial marker E-cadherin protein levels decreased, while mesenchymal marker N-cadherin and apoptin (caspase-3) expressions increased. These results were opposite in B3GALT5-AS1-silencing KFs (Figure 2F). These data suggested that B3GALT5-AS1 suppressed the proliferation, migration, and invasion of KFs, impeded epithelial-to-mesenchymal transition (EMT), and promoted cell apoptosis.

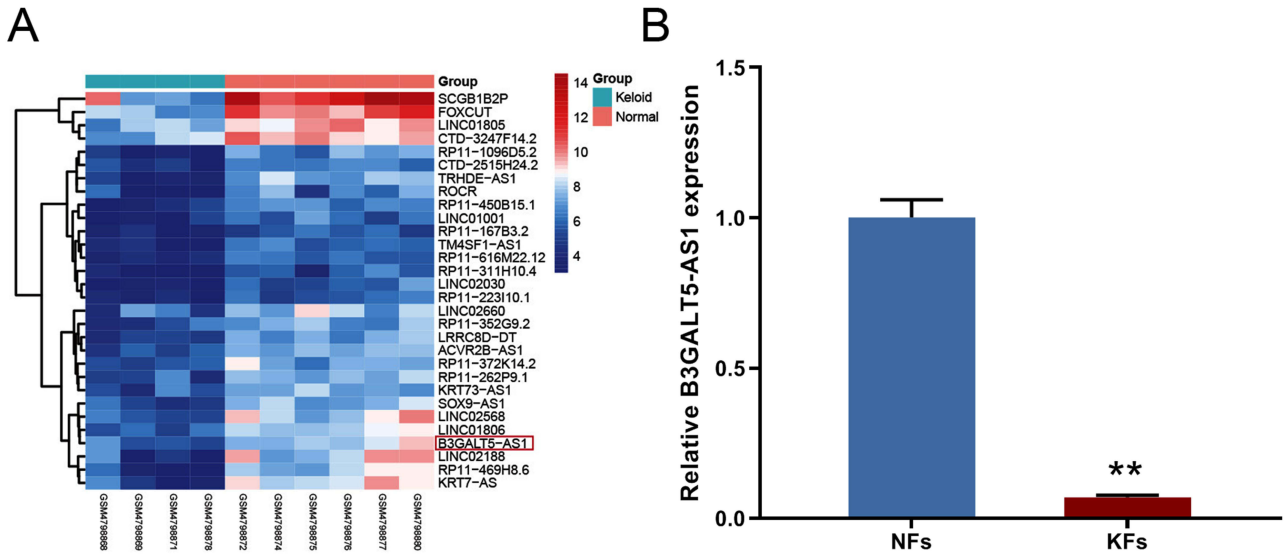


**Figure 1** B3GALT5-AS1 was down-regulated in keloid tissues and KFs. (**A**) Clustered heatmap illustrating top 30 down-regulated lncRNAs in keloid tissues (n = 4) compared to normal skin tissues (n = 6). The red box indicates B3GALT5-AS1. (**B**) qRT-PCR validation of B3GALT5-AS1 expression in KFs and NFs. The data are expressed as the mean ± SD.

**Note**: $^{**}p < 0.01$.

**Abbreviation**: KFs, primary keloid fibroblasts; NFs, primary normal fibroblasts.

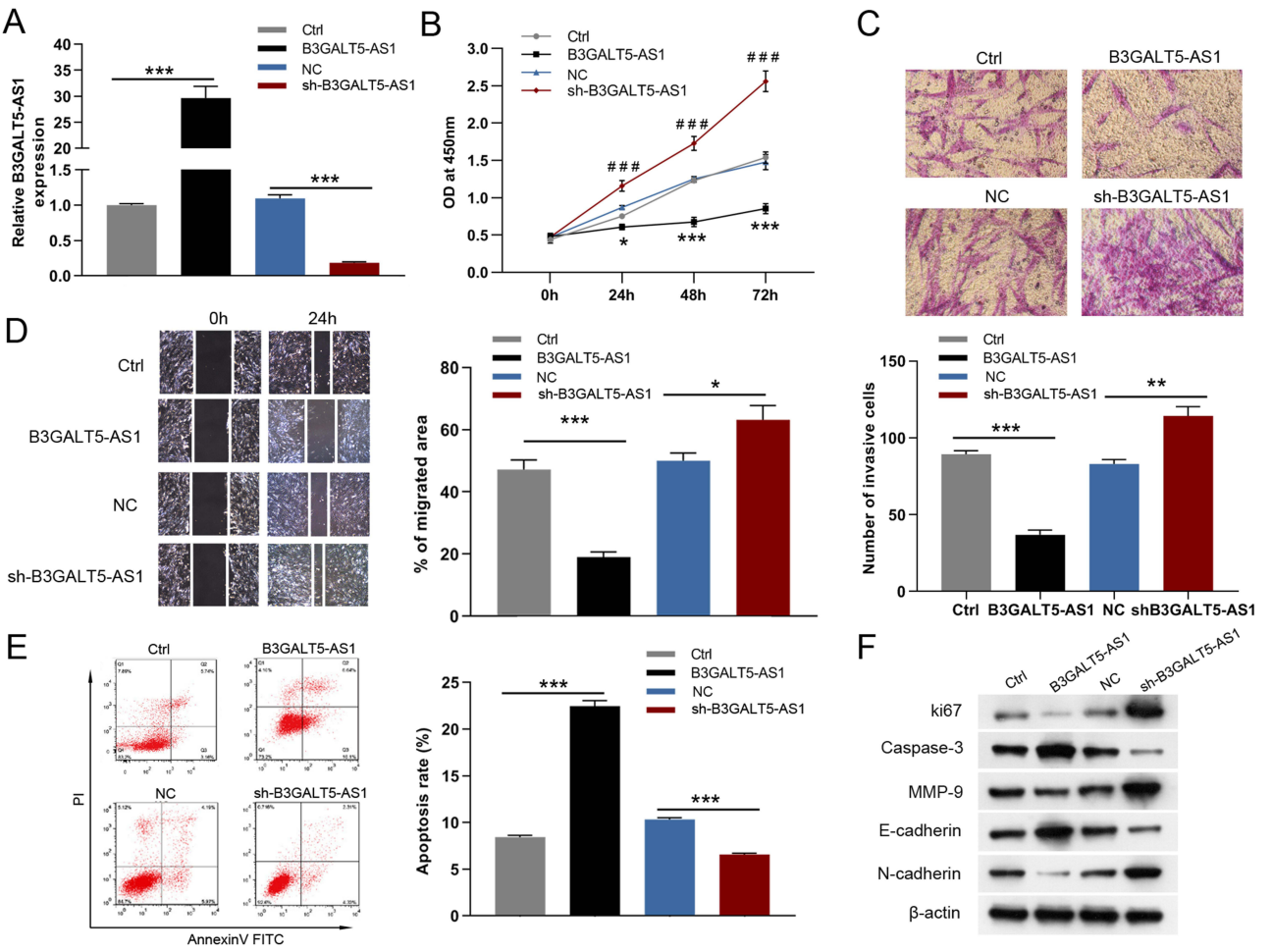


**Figure 2** B3GALT5-AS1 suppressed KFs proliferation and metastasis in vitro. (**A**) qRT-PCR detected the B3GALT5-AS1 expression in KFs to demonstrate the infected efficacy of overexpressing or knocking down B3GALT5-AS1. (**B**) MTT assay was used to measure the cell viability of KFs. (**C**) A transwell assay was applied to determine cell invasion. The invasive cells were visualized using crystal violet staining. (**D**) Migration abilities were measured using wound healing assay. (**E**) Cell apoptosis was determined using flow cytometry. (**F**) Western blotting assays were subjected to detect the effect of B3GALT5-AS1 overexpression or knockdown on the tumor proliferative marker, apoptin, migration-associated proteins, and EMT marker expressions, full-length blots are presented in Supplementary Figure 1. The P-value was determined using Student's t-tests. The data are expressed as the mean ± SD.

**Notes**: $^{*}p < 0.05$, $^{**}p < 0.01$, $^{***}p < 0.001$ and $^{\#\#\#}p < 0.001$.

**Abbreviation**: *KFs, primary keloid fibroblasts; B3GALT5-AS1, B3GALT5-AS1-overexpressed KFs; Ctrl, control of B3GALT5-AS1 overexpression; sh-B3GALT5-AS1, knockdown of B3GALT5-AS1 in KFs; NC, control of sh-B3GALT5-AS1*.

## B3GALT5-AS1 Inhibited Proliferation and Invasion of KFs Through Repressing Glycolysis Pathway

Some evidence suggests that tumor cell proliferation and metastasis are associated with glycolysis, which can produce lactic acid and alter the microenvironment of cells.[11–13] We examined glucose consumption, lactate production, and the ECAR and OCR in KFs in response to B3GALT5-AS1 knockdown or overexpression. Expectedly, B3GALT5-AS1 overexpression remarkably decreased glucose uptake, glycolysis, and lactate production of cells, while B3GALT5-AS1 knockdown significantly increased glucose consumption, glycolytic capacity, and lactate production of cells (Figures 3A–C). Meanwhile, opposite results were witnessed in OCR measurement (Figure 3D). The glycolysis inhibitor 2-DG was applied to block glycolysis signaling. B3GALT5-AS1 knockdown promoted cell proliferation and invasion, but this effect disappeared after treatment with 2-DG (Figures 3E and F). These data imply that B3GALT5-AS1 may repress the proliferation and invasion of KFs by inhibiting glycolysis.

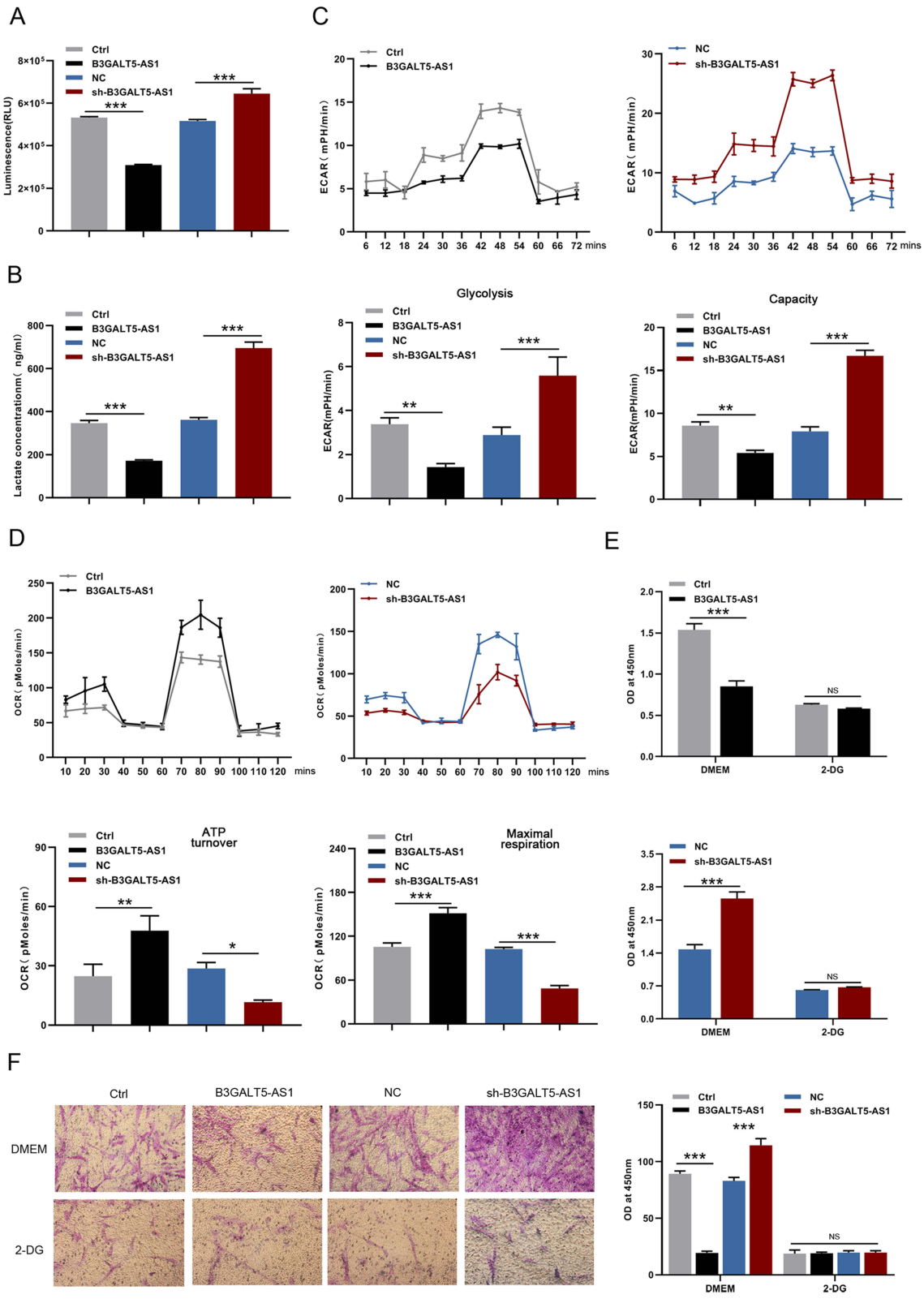


**Figure 3** B3GALT5-AS1 inhibited the proliferation and invasion of KFs by repressing glycolysis. (**A**) The glucose consumption of KFs was examined in response to B3GALT5-AS1 overexpression or knockdown. (**B**) The lactate production in KFs was measured after B3GALT5-AS1 overexpression or knockdown. The ECAR (**C**) and OCR (**D**) in KFs were examined using Seahorse XF assay. (**E**) The glycolysis 2-DG attenuated weakened the effect of B3GALT5-AS1 on KFs proliferation. (**F**) The inhibition of B3GALT5-AS1 on cell invasion was restrained by 2-DG. The data are expressed as the mean ± SD. *$p < 0.05$, **$p < 0.01$ and ***$p < 0.001$. NS, no significant difference. *KFs, primary keloid fibroblasts; B3GALT5-AS1, B3GALT5-AS1-overexpressed KFs; Ctrl, control of B3GALT5-AS1 overexpression; sh-B3GALT5-AS1, knockdown of B3GALT5-AS1 in KFs; NC, control of sh-B3GALT5-AS1.*

## B3GALT5-AS1 Interacted with HuR Leading to Its Degradation

Initially, we searched the lncLocator database to predict the potential location of B3GALT5-AS1 in cells to investigate the molecular mechanism of B3GALT5-AS1 in KFs proliferation and invasion (Figure 4A). Then, FISH experiment revealed that the Cy3-labeled B3GALT5-AS1 probe was specifically captured in cytoplasm of KFs (Figure 4B). The distribution of nuclear and cytoplasmic RNA also illustrated that B3GALT5-AS1 was localized predominantly in cytoplasm of fibroblasts (Figure 4C), suggesting that B3GALT5-AS1 might directly bind to cytoplasmic proteins and exert biologically function. We used the online databases, including EnCOR2 and catRAPID, to screen the potential B3GALT5-AS1-binding proteins and discovered that HuR may interact with B3GALT5-AS1 directly. Then, the RNA pull-down and RIP assays confirmed the combination of B3GALT5-AS1 with HuR (Figure 4D).

The qRT-PCR and Western blotting experiments were performed to determine the association between B3GALT5-AS1 and HuR. Interestingly, B3GALT5-AS1 overexpression in KFs down-regulated the HuR protein expression but did not significantly reduce its mRNA level. Similarly, silencing B3GALT5-AS1 in KFs up-regulated HuR protein expression but did not increase its mRNA level (Figure 4E), indicating that B3GALT5-AS1 regulates HuR protein levels rather than transcriptional signaling. B3GALT5-AS1 was separated into nine fragments to explore the locus that can bind to HuR. Among which only F2 can interact with HuR (Figure 4F). Moreover, the interaction was blocked after changing the gene sequence of F2, suggesting that F2 is the core active fragment of B3GALT5-AS1 (Figures 4G and H).

We treated B3GALT5-AS1-silenced KFs with CHX to impede protein synthesis and further investigate whether B3GALT5-AS1 regulates HuR expression by affecting protein stability. The cells also received proteasome inhibitor MG132 or lysosome inhibitor chloroquine. The results revealed that the HuR protein levels were higher in B3GALT5-AS1 knockdown KFs than NC groups, and MG132 could partly reverse HuR degradation, illustrating that its degradation may involve the ubiquitin-dependent proteasome system (Figure 4I). The ubiquitination of HuR could be facilitated by silencing B3GALT5-AS1 (Figure 4J). The β-Trcp1, a type of E3 ubiquitin ligase, could specifically target HuR and activate its ubiquitination.[14] Thus, we performed the co-immunoprecipitation experiment and verified that B3GALT5-AS1 overexpression promoted the interaction between HuR and β-Trcp1 in KFs (Figure 4K). We concluded that B3GALT5-AS1 can interact with HuR and degrade it via regulating β-Trcp1-mediated ubiquitination.

## B3GALT5-AS1 Degraded HuR to Repress KFs Proliferation and Metastasis in vitro

Next, we investigated the rescue ability of HuR on the inhibitory effects of B3GALT5-AS1 on KFs. In this part, B3GALT5-AS1 overexpressing KFs were transfected with or without HuR plasmid, and the transfection efficiency was detected by Western blotting (Figure 5A). Moreover, HuR overexpression significantly reversed the inhibitory effects of B3GALT5-AS1 on cell viability, migration, and invasion (Figures 5B–D). Furthermore, HuR up-regulation abolished the B3GALT5-AS1-induced KFs apoptosis (Figure 5E). The changes in the tumor proliferative marker, apoptin, migration-related protein, and EMT marker expressions in B3GALT5-AS1 overexpression KFs were rescued after HuR overexpression (Figure 5F). Collectively, these results demonstrated that B3GALT5-AS1 regulated KFs proliferation, migration, and apoptosis by attenuating HuR protein expression.

## HuR Attenuated the Inhibitory Effect of B3GALT5-AS1 on Glycolysis in KFs

Glucose uptake and lactate production measurements were performed to determine whether HuR has the rescue effect in response to B3GALT5-AS1-induced glycolysis inhibition in KFs. The reduced glucose consumption and lactate concentration induced by B3GALT5-AS1 overexpression were abrogated following HuR overexpression (Figures 6A and B). According to ECAR assay, HuR increased the glycolytic capacity that was decreased by B3GALT5-AS1 (Figure 6C). Similarly, increased ATP turnover and maximal respiration in B3GALT5-AS1 overexpressing KFs was diminished by HuR overexpression (Figure 6D). Overall, these findings illustrated that HuR could alleviate the glycolysis inhibition caused by B3GALT5-AS1.

# Discussion

The aggressive proliferation of fibroblasts and excessive extracellular matrix deposition are responsible for keloid development, while the molecular mechanisms are still unclear. Current treatment modalities, including surgical

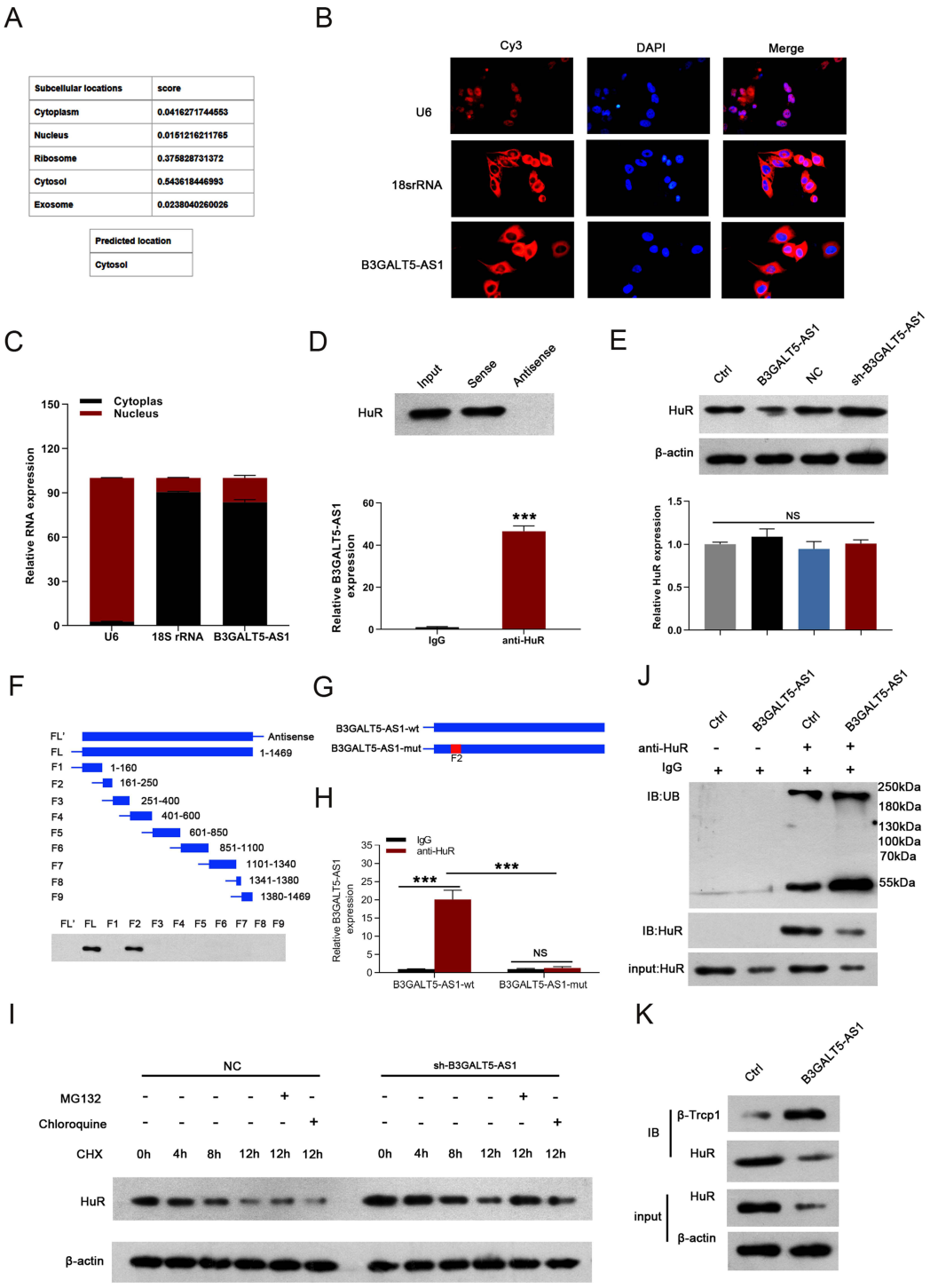


**Figure 4** B3GALT5-AS1 interacted with HuR leading to its degradation. (**A**) The result of the lncLocator database revealed that B3GALT5-AS1 is localized predominantly in the cytoplasm. (**B**) The FISH assay identified the subcellular location of B3GALT5-AS1 in KFs. (**C**) qRT-PCR experiments demonstrated that B3GALT5-AS1 expression was primarily distributed in cytoplasm relative to the nucleus of KFs. (**D**) RNA pull-down and RIP assays verified the combination of B3GALT5-AS1 with HuR in KFs. (**E**) qRT-PCR and Western blotting determined the HuR mRNA and protein expression levels in KFs infected with B3GALT5-AS1 plasmid, si-B3GALT5-AS1, or their corresponding control. (**F**) Schematic structures of B3GALT5-AS1 and nine fragments. RIP experiments confirmed the interaction of F2 and HuR. (**G**) Design of B3GALT5-AS1 mutation. (**H**) RIP experiment of HUR with B3GALT5-AS1-wt or B3GALT5-AS1-mut. (**I**) Western blotting was applied to detect the effect of CHX treatment with or without MG 132 or chloroquine on attenuated HuR protein levels by B3GALT5-AS1 knockdown in KFs, full-length blots are presented in Supplementary Figure 1. (**J**) Ubiquitination experiments were adopted to determine the HuR degradation in KFs infected with sh-B3GALT5-AS1 or NC lentiviruses after treatment with MG 132. (**K**) Co-immunoprecipitation experiment was performed to evaluate the interaction between β-Trcp1 and HUR. ***$p < 0.001$. NS, no significant difference. *KFs, primary keloid fibroblasts; B3GALT5-AS1, B3GALT5-AS1-overexpressed KFs; Ctrl, control of B3GALT5-AS1 overexpression; sh-B3GALT5-AS1, knockdown of B3GALT5-AS1 in KFs; NC, control of sh-B3GALT5-AS1.*

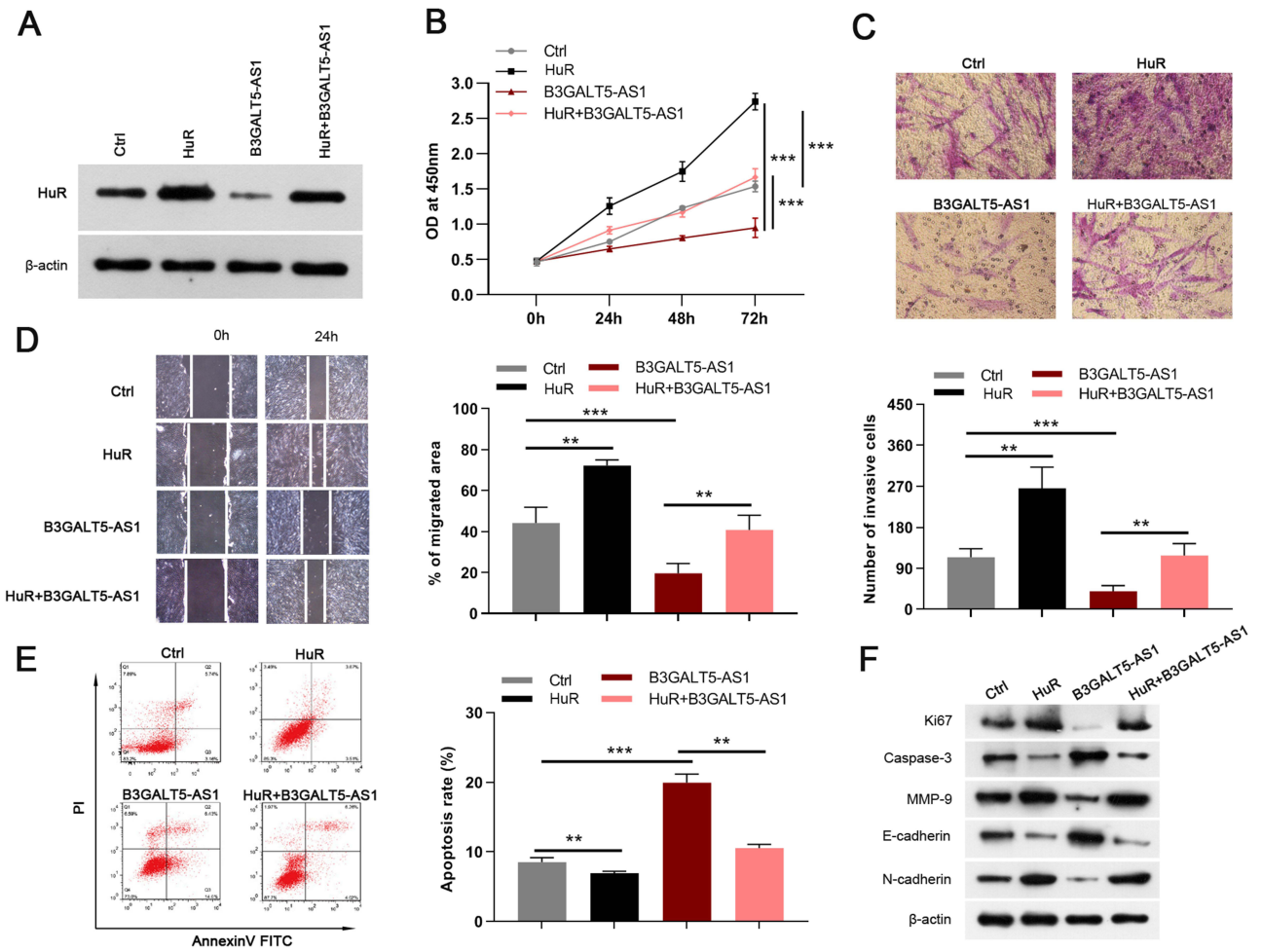


**Figure 5** B3GALT5-AS1 degraded HuR to repress KFs proliferation and metastasis in vitro. (**A**) Western blotting detected the HuR protein expression in KFs after overexpressing HuR and B3GALT5-AS1. (**B-D**) MTT, Transwell, and wound healing assays illustrated that the inhibitory effects of B3GALT5-AS1 overexpression on the proliferation, invasion, and migration of KFs were significantly abolished by HuR overexpression. (**E**) HuR up-regulation suppressed cell apoptosis induced by B3GALT5-AS1 overexpression. (**F**) Western blotting analysis of Ki67, Caspase-3, MMP-9, E-cadherin, and N-cadherin protein expression, full-length blots are presented in Supplementary Figure 1. The data are expressed as the mean ± SD. $^{**}p < 0.01$, and $^{***}p < 0.001$. *KFs, primary keloid fibroblasts; B3GALT5-AS1, B3GALT5-AS1-overexpressed KFs; Ctrl, control of B3GALT5-AS1 or HuR overexpression; HuR, HuR-overexpressed KFs; HuR+ B3GALT5-AS1, KFs co-overexpressing HuR and B3GALT5-AS1.*

resection, laser therapy, and radiation therapy, cannot provide optimal impacts for keloid treatment; thus, developing effective targets with high specificity and sensitivity is essential.[1,15] Here, we found that B3GALT5-AS1 was down-regulated in keloid tissues and KFs. Overexpression of B3GALT5-AS1 suppressed cell proliferation and metastasis via inhibiting glycolysis in KFs. Further investigations revealed that B3GALT5-AS1 bound to HuR and reduced its stability through promoting its ubiquitination and degradation at post-translational level.

B3GALT5-AS1, located in Chr21q22.2, was first identified as a down-regulated lncRNA in colon cancer tissues.[16] Afterward, the clinicopathological feature and biological functions of B3GALT5-AS1 have been investigated in different cancer types, where B3GALT5-AS1 exhibits adverse regulatory effects in tumor progression.[17–19] Increased B3GALT5-AS1 expression in colon cancer could inhibit colon cancer liver metastasis by activating B3GALT5-AS1/miR-203/EMT axis.[20] However, the B3GALT5-AS1 in gastric cancer presented oncogenic activities, including facilitating cell proliferation, migration, invasion, and EMT.[21] Our study demonstrated that a high B3GALT5-AS1 expression was required to suppress cell proliferation, inhibit migration, and increase cell apoptosis in KFs.

When searching the subcellular location of B3GALT5-AS1, we discovered that B3GALT5-AS1 was mainly distributed in the cytosol (Figure 4A). HuR plays an oncogenic role in tumor progression through its nuclear/cytoplasmic shuttling.[22] Increase in cytoplasmic HuR expression contributes to aberrant transcripts linked to tumor genome, suppression of cell-cycle

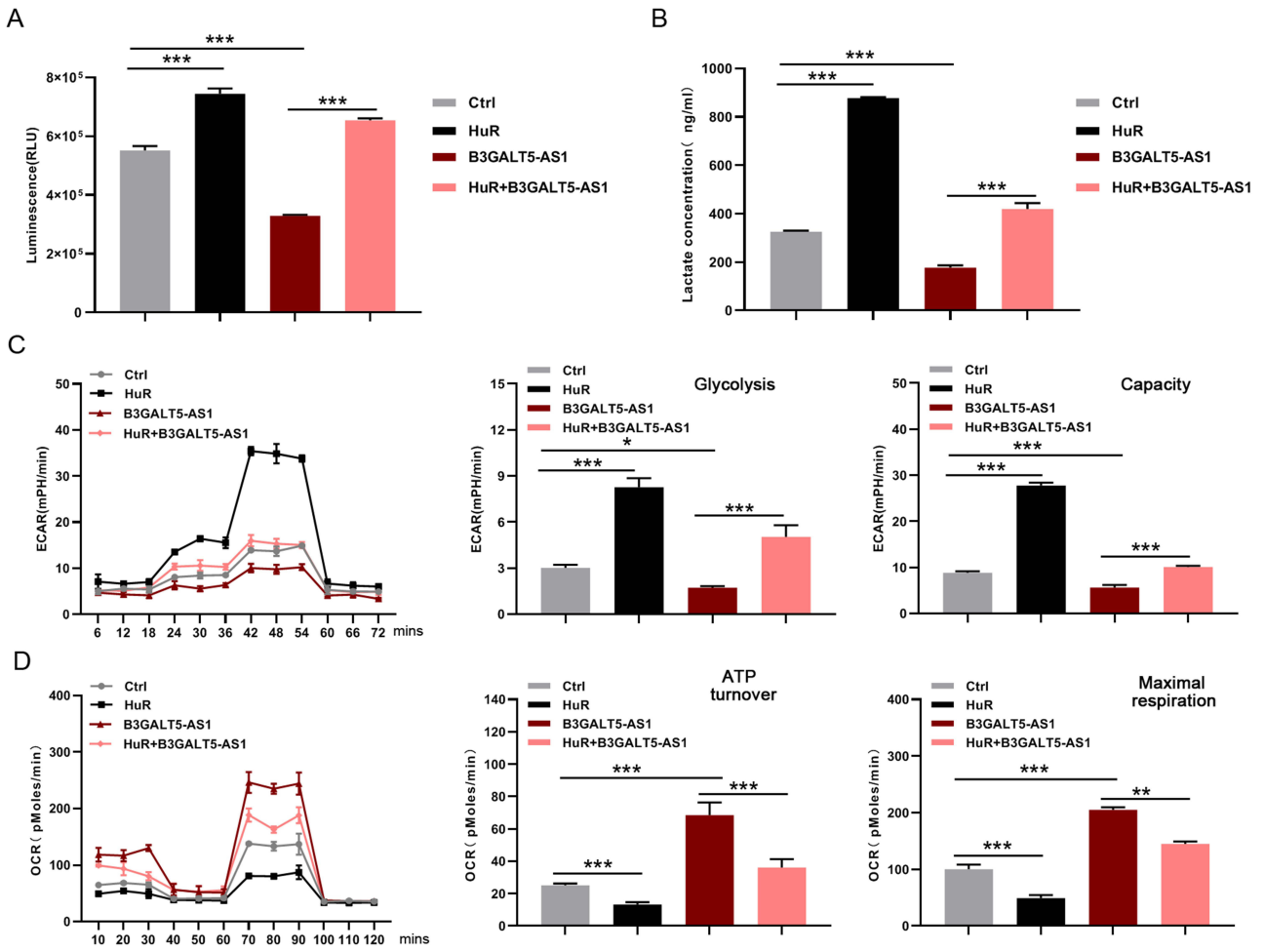


**Figure 6** HuR attenuated the inhibitory effect of B3GALT5-AS1 on glycolysis in KFs. (**A**) The glucose consumption, lactate production (**B**), ECAR (**C**), and OCR (**D**) of KFs were detected after HuR, B3GALT5-AS1, or both HuR and B3GALT5-AS1 overexpression. The data are expressed as the mean ± SD. *$p < 0.05$, **$p < 0.01$, and ***$p < 0.001$. *KFs, primary keloid fibroblasts; B3GALT5-AS1, B3GALT5-AS1-overexpressed KFs; Ctrl, control of B3GALT5-AS1 or HuR overexpression; HuR, HuR-overexpressed KFs; HuR+B3GALT5-AS1, KFs co-overexpressing HuR and B3GALT5-AS1.*

progression, and cell apoptosis.[22] Many evidences have demonstrated that lncRNAs show great inhibitory effects in oncogenesis by binding to HuR and modulating its stability.[23–25] For instance, OCC-1 suppressed cell growth in colorectal cancer through promoting β-Trcp1-mediated degradation of HuR.[23] More recently, ASB16-AS1 and OIP5-AS1 have also been reported to inhibit tumor cell growth via accelerating ubiquitination of HuR.[24,25] Herein, we predicted that B3GALT5-AS1 may interact with HuR by analyzing online databases and further verified the B3GALT5-AS1 locus interacting with HuR. In this study, B3GALT5-AS1 regulates the level of HuR protein via accelerating its ubiquitination and degradation. Conversely HuR overexpression improved the inhibition of B3GALT5-AS1 on KFs pathological procedure. Our findings elucidated an HuR-associated regulatory mechanism in keloid development, where B3GALT5-AS1 acted as an anti-tumor candidate.

## Conclusion

In the current study, we revealed that the level of B3GALT5-AS1 was significantly decreased in keloid tissues. Mechanistically, B3GALT5-AS1 triggered β-Trcp1-mediated HuR degradation and inhibited glycolysis in KFs, repressing cell proliferation and metastasis. Collectively, these results illustrated that B3GALT5-AS1 might be a promising inhibitor for development of therapeutic strategies against keloid disorder.

## Data Sharing Statement

The data that support the findings of this study are available from the corresponding author upon reasonable request.

## Ethical Approval

This study was approved by the Ethics Committee for Huizhou Municipal Central Hospital (kyll2021240). The study was performed in accordance with the Declaration of Helsinki, the Belmont Report and ICH-GCP. Moreover, informed consent was obtained from all patients.

## Author Contributions

All authors made a significant contribution to the work reported, whether that is in the conception, study design, execution, acquisition of data, analysis and interpretation, or in all these areas; took part in drafting, revising or critically reviewing the article; gave final approval of the version to be published; have agreed on the journal to which the article has been submitted; and agree to be accountable for all aspects of the work.

## Funding

This work was supported by 2022 Guangdong Medical Research Fund (A2022174).

## Disclosure

All authors declare no conflicts of interest in this work.

## References

1. Bran GM, Goessler UR, Hormann K, Riedel F, Sadick H. Keloids: current concepts of pathogenesis (review). *Int J Mol Med*. 2009;24(3):283–293. doi:10.3892/ijmm_00000231
2. Lee HJ, Jang YJ. Recent understandings of biology, prophylaxis and treatment strategies for hypertrophic scars and keloids. *Int J Mol Sci*. 2018;19(3).1
3. Slemp AE, Kirschner RE. Keloids and scars: a review of keloids and scars, their pathogenesis, risk factors, and management. *Curr Opin Pediatr*. 2006;18(4):396–402. doi:10.1097/01.mop.0000236389.41462.ef
4. Jiang MC, Ni JJ, Cui WY, Wang BY, Zhuo W. Emerging roles of lncRNA in cancer and therapeutic opportunities. *Am J Cancer Res*. 2019;9(7):1354–1366.
5. Morris KV, Mattick JS. The rise of regulatory RNA. *Nat Rev Genet*. 2014;15(6):423–437. doi:10.1038/nrg3722
6. Li Y, Egranov SD, Yang L, Lin C. Molecular mechanisms of long noncoding RNAs-mediated cancer metastasis. *Genes Chromosomes Cancer*. 2019;58(4):200–207. doi:10.1002/gcc.22691
7. Lv W, Ren Y, Hou K, et al. Epigenetic modification mechanisms involved in keloid: current status and prospect. *Clin Clin Epigenet*. 2020;12(1):183. doi:10.1186/s13148-020-00981-8
8. He Y, Deng Z, Alghamdi M, Lu L, Fear MW, He L. From genetics to epigenetics: new insights into keloid scarring. *Cell Prolif*. 2017;50(2). doi:10.1111/cpr.12326
9. Wang Z, Feng C, Song K, Qi Z, Huang W, Wang Y. lncRNA-H19/miR-29a axis affected the viability and apoptosis of keloid fibroblasts through acting upon COL1A1 signaling. *J Cell Biochem*. 2020;121(11):4364–4376. doi:10.1002/jcb.29649
10. Jin J, Jia ZH, Luo XH, Zhai HF. Long non-coding RNA HOXA11-AS accelerates the progression of keloid formation via miR-124-3p/TGFbetaR1 axis. *Cell Cycle*. 2020;19(2):218–232. doi:10.1080/15384101.2019.1706921
11. Du JY, Wang LF, Wang Q, Yu LD. miR-26b inhibits proliferation, migration, invasion and apoptosis induction via the downregulation of 6-phosphofructo-2-kinase/fructose-2,6-bisphosphatase-3 driven glycolysis in osteosarcoma cells. *Oncol Rep*. 2015;33(4):1890–1898. doi:10.3892/or.2015.3797
12. Liu Y, Tong L, Luo Y, Li X, Chen G, Wang Y. Resveratrol inhibits the proliferation and induces the apoptosis in ovarian cancer cells via inhibiting glycolysis and targeting AMPK/mTOR signaling pathway. *J Cell Biochem*. 2018;119(7):6162–6172. doi:10.1002/jcb.26822
13. Zhou J, Zhang S, Chen Z, He Z, Xu Y, Li Z. CircRNA-ENO1 promoted glycolysis and tumor progression in lung adenocarcinoma through upregulating its host gene ENO1. *Cell Death Dis*. 2019;10(12):885. doi:10.1038/s41419-019-2127-7
14. Chu PC, Chuang HC, Kulp SK, Chen CS. The mRNA-stabilizing factor HuR protein is targeted by beta-TrCP protein for degradation in response to glycolysis inhibition. *J Biol Chem*. 2012;287(52):43639–43650. doi:10.1074/jbc.M112.393678
15. Mari W, Alsabri SG, Tabal N, Younes S, Sherif A, Simman R. Novel insights on understanding of keloid scar: article review. *J Am Coll Clin Wound Spec*. 2015;7(1–3):1–7. doi:10.1016/j.jccw.2016.10.001
16. Feng W, Zong W, Li Y, Shen X, Cui X, Ju S. Abnormally expressed long noncoding RNA B3GALT5-AS1 may serve as a biomarker for the diagnostic and prognostic of gastric cancer. *J Cell Biochem*. 2020;121(1):557–565. doi:10.1002/jcb.29296
17. Ding Y, Feng W, Ge JK, et al. Serum level of long noncoding RNA B3GALT5-AS1 as a diagnostic biomarker of colorectal cancer. *Future Oncol*. 2020;16(13):827–835. doi:10.2217/fon-2019-0820
18. Chen S, Shen X. Long noncoding RNAs: functions and mechanisms in colon cancer. *Mol Cancer*. 2020;19(1):167. doi:10.1186/s12943-020-01287-2
19. Wang L, Zhao X, Wang Y. The pivotal role and mechanism of long non-coding RNA B3GALT5-AS1 in the diagnosis of acute pancreatitis. *Artif Cells Nanomed Biotechnol*. 2019;47(1):2307–2315. doi:10.1080/21691401.2019.1623231
20. Wang L, Wei Z, Wu K, et al. Long noncoding RNA B3GALT5-AS1 suppresses colon cancer liver metastasis via repressing microRNA-203. *Aging*. 2018;10(12):3662–3682. doi:10.18632/aging.101628
21. Wang P, Sun GB, Dou GX, Wang BQ. Long non-coding RNA B3GALT5-AS1 contributes to the progression of gastric cancer via interacting with CSNK2A1. *Exp Ther Med*. 2021;22(3):927. doi:10.3892/etm.2021.10359

22. Filippova N, Yang X, Ananthan S, et al. Targeting the HuR oncogenic role with a new class of cytoplasmic dimerization inhibitors. *Cancer Res*. 2021;81(8):2220–2233. doi:10.1158/0008-5472.CAN-20-2858
23. Lan Y, Xiao X, He Z, et al. Long noncoding RNA OCC-1 suppresses cell growth through destabilizing HuR protein in colorectal cancer. *Nucleic Acids Res*. 2018;46(11):5809–5821. doi:10.1093/nar/gky214
24. Long B, Yang X, Xu X, et al. Long noncoding RNA ASB16-AS1 inhibits adrenocortical carcinoma cell growth by promoting ubiquitination of RNA-binding protein HuR. *Cell Death Dis*. 2020;11(11):995. doi:10.1038/s41419-020-03205-2
25. Wang Y, Lin C, Liu Y. Molecular mechanism of miR-34b-5p and RNA binding protein HuR binding to lncRNA OIP5-AS1 in colon cancer cells. *Cancer Genet Ther*. 2022;29(5):612–624. doi:10.1038/s41417-021-00342-4